# A.c. Polarographic Study of Ion Transfer at the Water/Nitrobenzene Interface

Toshiyuki Osakai, Tadaaki Kakutani, and Mitsugi Senda*
*Department of Agricultural Chemistry, Faculty of Agriculture, Kyoto University, Sakyo-ku, Kyoto 606*
(Received August 22, 1983)

The transfer of tetramethylammonium ($TMA^+$) ion across the interface between a 0.1 mol $dm^{-3}$ LiCl aqueous solution and a 0.1 mol $dm^{-3}$ tetrabutylammonium tetraphenylborate nitrobenzene solution was investigated by means of phase-selective a.c. polarography. In recording the a.c. polarographic current a two-electrode cell system was used and the ohmic drop due to solution resistance in the cell was compensated for by positive feedback. The ion-transfer admittance *vs.* potential curves were determined in the a.c. frequency range between 10 and 100 Hz and the kinetic parameters of the $TMA^+$-ion transfer across the water/nitrobenzene interface were determined.

Kinetics of the charge (ion or electron) transfer at the interface between two immiscible electrolyte solutions has been studied by several authors using electrochemical techniques. Gavach and his coworkers have employed chronopotentiometry[1-3] and impedance measurement methods[1] to determine the kinetic parameters of the transfer of alkylammonium ions at the water/nitrobenzene interface. Recently, Koczorowsky and Geblewicz[4] have also applied chronopotentiometry to the kinetic study of the transfer of tetrabutylammonium ion at the water/1,2-dichloroethane interface. On the other hand, Samec *et al.* have employed cyclic voltammetry, with or without convolution analysis, for the kinetic studies of the transfer of $Cs^+$ ion at the water/nitrobenzene interface[5,6] and the transfer of alkaline earth metal cations facilitated by synthetic neutral carriers at the water/nitrobenzene interface,[7] and also the electron transfer between ferrocene in nitrobenzene and hexacyanoferrate(II) in water.[6]

In this work we have applied a phase-selective a.c. polarographic technique to the study of the kinetics of ion (tetramethylammonium ion) transfer at the water/nitrobenzene interface; an a.c. voltage of small amplitude was superimposed on a linear sweep voltage applied to the interface, and the real and imaginary components of the resulting alternating current were recorded against the applied linear sweep voltage in the frequency range between 10 and 100 Hz and in the concentration range of transferring ion between $0.15\times10^{-3}$ and $0.50\times10^{-3}$ mol $dm^{-3}$. In recording phase-selective a.c. polarographic curves we used a two-electrode cell system and the ohmic drop due to the solution resistance in the cell was compensated for by a positive feedback circuit. The recorded phase-selective a.c. polarographic currents were transformed into the admittance of the test interface and the latter was corrected for the admittance of the base aqueous solution/base nitrobenzene solution interface to give the admittance due to the ion transfer at the interface. The resulting ion-transfer admittance *vs.* potential curves were analysed using the conventional theory of a.c. polarography, and the kinetic parameters of the ion transfer at the water/nitrobenzene interface were determined.

## Experimental

*Chemicals.* The tetramethylammonium chloride (TMACl) was analytical grade (Wako Pure Chemical Industries, Ltd.), and used as received. The tetrabutylammonium chloride (TBACl) was analytical grade (Nakarai Chemicals Co.), and was purified as previously described.[8] The concentrations of TMACl and TBACl were determined by potentiometric titration with a standard silver nitrate solution. The analytical grade nitrobenzene (Nakarai) was distilled under reduced pressure; the middle 60% of the distillate was collected and shaken with active alumina overnight; after filtration of the suspension, the filtrate was washed with triply distilled water. The nitrobenzene solution of tetrabutylammonium tetraphenylborate (TBATPB) was prepared in the dark immediately before use. The other chemicals and the preparation of the aqueous solution have been described elsewhere.[9]

*Electrolytic Cell.* The electrolytic cell assembly is shown in Fig. 1. A glass tube A, which was filled with a 0.1 mol $dm^{-3}$ LiCl aqueous solution containing $(0.15-0.50)\times10^{-3}$ mol $dm^{-3}$ TMACl, was dipped into a 0.1 mol $dm^{-3}$ TBATPB nitrobenzene solution. The test interface was formed at the end of the glass tube A with an area of 0.159 $cm^2$. A reproducible, flat water/nitrobenzene interface was formed by treating the edge and the outer surface of the glass tube with dimethyldichlorosilane.[9,10] The test interface was

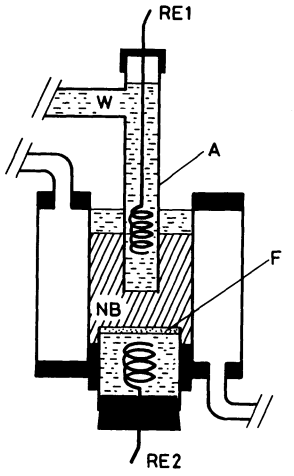


Fig. 1. Electrolytic cell. W, water phase; NB, nitrobenzene phase; A, glass tube; RE1 and RE2, reference electrodes; F, sintered glass.

renewed for each measurement of a single a.c. polarogram. The cell was water-jacketted at 25±0.1 °C.

The reference electrode for the nitrobenzene phase, RE2, was an Ag/AgCl/0.1 mol dm$^{-3}$ TBACl (water) electrode with a large surface area (>6 cm$^2$), which was connected to the nitrobenzene phase through sintered glass. The other reference electrode for the aqueous phase, RE1, was an Ag/AgCl electrode with a large surface area (>4 cm$^2$), which was immersed in the aqueous phase. Accordingly, the cell to be studied can be expressed by:

$$\begin{array}{l} \qquad\qquad\qquad\quad \text{I} \qquad\qquad\quad \text{II} \\ \text{(RE2) Ag}\,|\,\text{AgCl}\,|\,0.1\ \text{mol dm}^{-3}\ \text{TBACl}\ \text{(W)}\,|\,0.1\ \text{mol dm}^{-3}\ \text{TBATPB}\ \text{(N)} \\ \qquad\qquad\qquad\quad \text{III} \\ \qquad |\,(0.15\text{—}0.50)\times 10^{-3}\ \text{mol dm}^{-3}\ \text{TMACl} \\ \qquad\qquad\qquad\qquad\qquad\qquad\qquad\qquad\qquad\qquad \text{(W)} \\ \qquad\qquad + 0.1\ \text{mol dm}^{-3}\ \text{LiCl} \\ \qquad |\,\text{AgCl}\,|\,\text{Ag (RE1)}, \qquad\qquad\qquad\qquad\qquad\qquad\qquad\qquad\qquad\qquad \text{(A)} \end{array}$$

where (W) and (N) represent the aqueous and the nitrobenzene phases. The interface between phases I and II is nonpolarizable and the potential difference across the interface is determined by the activities of TBA$^+$ ion in the two phases.[9,10]

*Measurement of Solution Resistance.* In a.c. polarographic measurements, we adopted a two-electrode cell system in which the ohmic drop due to the solution resistance between RE1 and RE2, $R_u$, was compensated for by means of positive feedback (see Fig. 3). For exact compensation of the ohmic drop, the value of $R_u$ must be known accurately. We used a laboratory-made linear bridge[11] to determine $R_u$. Figure 2 shows the basic circuit of the bridge, which allowed accurate determination of resistance (a dummy cell resistance) using a 10 kHz a.c. generator with an error less than 10 Ω in the range between 0.5 and 5.0 kΩ. Determination of $R_u$ was made every time the test interface was renewed. For a representative cell, as shown in Fig. 1, $R_u$ was in the range between 1.41 and 1.54 kΩ.

*A.c. Polarographic Measurement.* The diagram of the basic electronic circuit for measurement of the interfacial impedance with a two-electrode cell system is shown in Fig. 3. The circuit bordered by broken lines is a conventional polarographic circuit (Yanako potentiostat PE21-TB2S). D.c. and a.c. voltages are generated by a sweep generator (Hokuto Denko HB-104) and an a.c. generator (YHP 3310B), respectively, and applied through $R_1$ to the summing point, $e_s$, of the inverting adder (OA1 and OA2), the output of which is applied to the terminal of RE1, while the terminal of RE2 is always held at virtual ground. The output voltage of OA3, $E_o$, is proportional to the current flowing through the cell, $i$, that is, $E_o=iR_i$. For the ohmic drop compensation, a part of this output voltage was fed back to the summing point. The feedback voltage was made equal to $\beta R_u i=\beta R_u E_o/R_i$ by adjusting a potentiometer, $R_c$, where $\beta$ is the fraction of positive feedback and $\beta=1$ for 100% positive feedback. The real (in-phase) and imaginary (out-of-phase) components of the a.c. polarographic current flowing through the cell were determined by a lock-in amplifier (NF LI-574) and recorded against the linear sweep voltage applied to the test interface, usually at the voltage scan rate of $v=5$ mV s$^{-1}$, using an X-Y

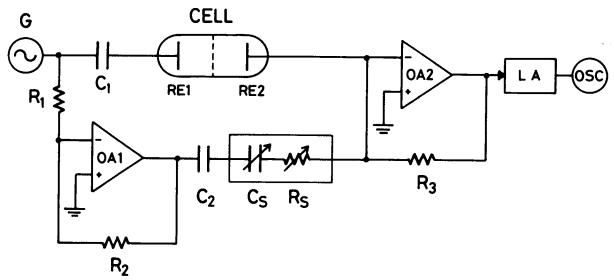


Fig. 2. Basic circuit of the linear bridge for measurement of the solution resistance. OA1 and OA2, operational amplifiers (Texas Instrument TLO82CP); G, a.c. generator (NF 572B); LA, lock-in amplifier (NF 572B); OSC, oscilloscope (Hitachi VC-801L); $R_s$ and $C_s$, decade resistor and decade capacitor; $R_1=R_2=43$ kΩ; $R_3=100$ kΩ; $C_1=C_2=1$ μF.

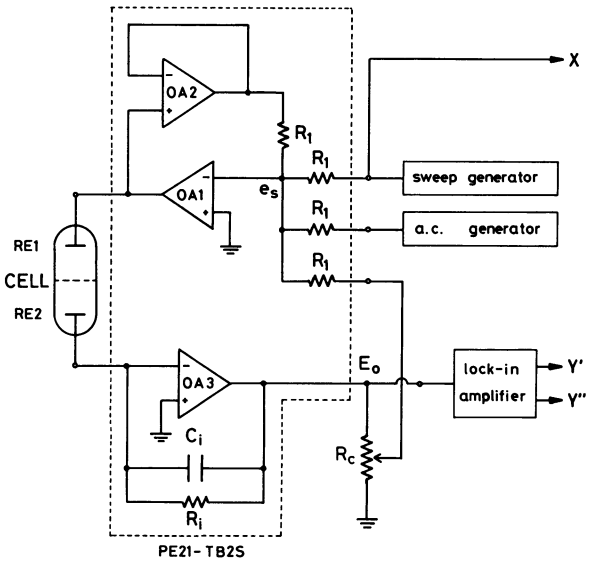


Fig. 3. Electronic circuit for d.c. and a.c. polarographic measurement with a two-electrode cell. X, Y′, and Y″, inputs of recorder; RE1 and RE2, reference electrodes; OA1 to OA3, operational amplifiers (Burr Brown 3112/12C); $R_i$, current-measuring resistor (10 kΩ); $C_i$, damping capacitor (1000 pF); $R_c$, potentiometer (1 kΩ); $R_1$, resistor (10 kΩ).

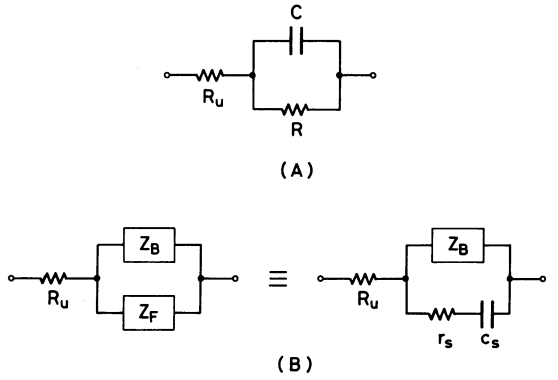


Fig. 4. (A) Dummy cell. $R$, $C$, and $R_u$ correspond, respectively, to the resistance and capacitance of the test interface, and the solution resistance. (B) Equivalent circuit of the cell. $R_u$, solution resistance; $Z_B$, base impedance; $Z_F=r_s-j(1/\omega c_s)$, ion-transfer impedance.

recorder (Watanabe WX4302). The magnitude of the superimposed a.c. voltage (usually 5 mV peak to peak) was calibrated by replacing the cell with a known capacitor and measuring the a.c. current flowing through the capacitor by the lock-in amplifier.

The measuring circuit was calibrated by a dummy cell, which consists of $R_u$=1.5 kΩ, $R$=0.2 to 2 kΩ, and $C$=2 to 20 μF, as shown in Fig. 4(A), in the a.c. frequency range of 10 to 100 Hz. The error in measuring the dummy admittance ($1/R$ and $\omega C$) with $\beta$ being equal to 1 was not negligible, especially at high frequencies. Accordingly, the measured or apparent admittance was corrected for the non-ideal dynamic response of the measuring circuit, where the response was represented, in the first approximation, by the gain function of $G=K/(1+\tau_a s)$ of the control amplifier (OA1) with other amplifiers functioning ideally. The residual error in the corrected admittance was less than 1, 3, and 6% at 10, 50, and 100 Hz, respectively, in the calibrated range of $R$ and $C$ of the dummy cell.

## Theoretical

In the following, the potential applied to cell A, $E$, is defined as the potential of RE1 against that of RE2, *i.e.*, $E=E_{RE1}-E_{RE2}$. The flow of the positive charge from the aqueous to the nitrobenzene phase is taken as the positive current.

*Interfacial Admittance.* The admittance of the test interface as determined by phase-selective a.c. polarography can be generally represented by:

$$Y_t = Y_t' + jY_t'', \tag{1}$$

where $j$ is an operator $j=(-1)^{1/2}$. Let the base admittance, that is, the admittance of the base aqueous solution/base nitrobenzene solution interface, be $Y_B=Y_B'+jY_B''$. Then the admittance due to the ion transfer $Y_F=Y_F'+jY_F''$ can be estimated by:

$$Y_F' = Y_t' - Y_B', \tag{2}$$

$$Y_F'' = Y_t'' - Y_B''. \tag{3}$$

Finally, the ion-transfer admittance, $Y_F$, is related to a series combination of resistance and capacitance, $r_s$ and $c_s$, due to the ion transfer (see Fig. 4(B)) by:

$$r_s = Y_F'/(Y_F'^2 + Y_F''^2), \tag{4}$$

$$1/\omega c_s = Y_F''/(Y_F'^2 + Y_F''^2), \tag{5}$$

where $\omega$ is the a.c. angular frequency ($\omega=2\pi f$, $f$ being the a.c. frequency).

*Ion-transfer Impedance.* We suppose that the ion-transfer current $I$ is a function of the surface concentrations of the ion in the aqueous and nitrobenzene phases, $C^W$ and $C^N$, and of the interfacial potential difference, $\Delta_N^W\phi$, or the potential applied to the cell, $E=\Delta_N^W\phi+\Delta E_{ref}$, where $\Delta E_{ref}$ is determined by the reference electrode system:[9]

$$I = I(E,C^W,C^N). \tag{6}$$

In this and the following equations the terms containing activity coefficients of the ions are neglected for the sake of simplicity. When a small a.c. voltage is superimposed on the d.c. potential, $E_{dc}$, the ion-transfer impedance, $r_s-j(1/\omega c_s)$ (see Fig. 4(B)), can be generally expressed, by analogy with the faradaic impedance of an electrode reaction,[12-14] by:

$$r_s = r_{ct} + r^W + r^N, \tag{7}$$

$$1/\omega c_s = x^W + x^N, \tag{8}$$

with

$$r_{ct} = 1/\left(\frac{\partial I}{\partial E}\right)_{dc}, \tag{9}$$

$$r^\alpha = \pm\left[\left(\frac{\partial I}{\partial C^\alpha}\right)_{dc}\Big/\left(\frac{\partial I}{\partial E}\right)_{dc}\right](h_r)^\alpha(1/zFA), \tag{10}$$

$$x^\alpha = \pm\left[\left(\frac{\partial I}{\partial C^\alpha}\right)_{dc}\Big/\left(\frac{\partial I}{\partial E}\right)_{dc}\right](h_y)^\alpha(1/zFA), \tag{11}$$

where the superscript $\alpha$ (=W and N) stands for the aqueous (W) and nitrobenzene (N) phases, and the upper and lower signs in Eqs. 10 and 11 apply to W and N, respectively; $z$ is the ionic valence, $F$ the Faraday and $A$ the surface area of the test interface. The expression $(\ )_{dc}$ means the partial differential coefficients with respect to the stated variable of Eq. 6 at $E=E_{dc}$, and $(h_r)^\alpha$ and $(h_y)^\alpha$ are the coefficients, which depend only on the mass transfer of the ion in the two phases and are given for semi-infinite linear diffusion by:

$$(h_r)^\alpha = (h_y)^\alpha = (2\omega D^\alpha)^{-1/2}, \tag{12}$$

where $D^\alpha$ is the diffusion coefficient of the ion in the $\alpha$ phase.

When the ion transfer is reversible or nernstian in d.c. cyclic voltammetry, the Nernst equation is valid for the d.c. components of surface concentration or the mean surface concentrations, $\bar{C}^W$ and $\bar{C}^N$:

$$E_{dc} = E^\circ + (RT/zF)\ln(\bar{C}^N/\bar{C}^W). \tag{13}$$

Here $E^\circ$ is the standard potential of the ion transfer at the test interface with respect to the reference electrode system in cell A and is defined by:

$$E^\circ = -\frac{\Delta G_{tr}^{\ominus,N\to W}}{zF} + \Delta E_{ref}, \tag{14}$$

where $\Delta G_{tr}^{\ominus,N\to W}$ is the standard Gibbs free energy of ion transfer from the nitrobenzene to the aqueous phase. Thus, we have $(\partial I/\partial C^W)_{dc}/(\partial I/\partial E)_{dc}=-(\partial E_{dc}/\partial \bar{C}^W)=(RT/zF)(1/\bar{C}^W)$ and $(\partial I/\partial C^N)_{dc}/(\partial I/\partial E)_{dc}=-(\partial E_{dc}/\partial \bar{C}^N)=-(RT/zF)(1/\bar{C}^N)$. For semi-infinite linear diffusion, we also have $(D^W)^{1/2}(C^{W,o}-\bar{C}^W)=(D^N)^{1/2}(\bar{C}^N-C^{N,o})$ where $C^{\alpha,o}$ is the bulk concentration of the ion in the $\alpha$ phase. Then we get from Eqs. 7 to 13, upon assuming that $C^{N,o}=0$:

$$r_s = (\sigma/\omega^{1/2})[1+(2\omega)^{1/2}\lambda^{-1}], \tag{15}$$

$$1/\omega c_s = \sigma/\omega^{1/2}, \tag{16}$$

where

$$\sigma = \frac{4RT\cosh^2(\xi/2)}{z^2F^2A(2D^W)^{1/2}C^{W,o}}, \tag{17}$$

$$\xi = zF(E_{dc} - E_{1/2}^r)/RT, \tag{18}$$

$$E_{1/2}^r = E^\circ + (RT/zF)\ln(D^W/D^N)^{1/2}, \tag{19}$$

and

$$\lambda = \frac{1}{zFA(D^W)^{1/2}}\left(\frac{\partial I}{\partial C^W}\right)_{dc} - \frac{1}{zFA(D^N)^{1/2}}\left(\frac{\partial I}{\partial C^N}\right)_{dc}. \tag{20}$$

Equations 15 and 16 can be rewritten as:

$$\lambda = (2\omega)^{1/2}/(r_s c_s \omega - 1). \quad (21)$$

For the sake of simplicity, we assume a simple linear kinetic equation:

$$I = zFA(\vec{k}C^W - \overleftarrow{k}C^N), \quad (22)$$

where $\vec{k}$ and $\overleftarrow{k}$ are the rate constants of the ion transfer from the aqueous to the nitrobenzene phase and from the nitrobenzene to the aqueous phase, respectively. We further assume Butler-Volmer type equations for $\vec{k}$ and $\overleftarrow{k}$:

$$\vec{k} = k_s \exp[\vec{\alpha}zF(E_{dc}-E^\circ)/RT], \quad (23)$$

$$\overleftarrow{k} = k_s \exp[-\overleftarrow{\alpha}zF(E_{dc}-E^\circ)/RT], \quad (24)$$

where $k_s$ is the standard rate constant; $\vec{\alpha}$ and $\overleftarrow{\alpha}$ ($\vec{\alpha}+\overleftarrow{\alpha}=1$) are the transfer coefficients. Then Eq. 20 can be written as:

$$\lambda = \frac{\vec{k}}{(D^W)^{1/2}} + \frac{\overleftarrow{k}}{(D^N)^{1/2}}$$

$$= A[\exp(\vec{\alpha}\xi) + \exp(-\overleftarrow{\alpha}\xi)], \quad (25)$$

with

$$A = k_s\left(\frac{1}{(D^W)^{1/2}}\right)^{\overleftarrow{\alpha}}\left(\frac{1}{(D^N)^{1/2}}\right)^{\vec{\alpha}}, \quad (26)$$

Equation 25 can also be rewritten as:

$$\ln[\lambda/(1+\exp(-\xi))] = \ln A + \vec{\alpha}\xi. \quad (27)$$

## Results and Discussion

*Cyclic Voltammetry of $TMA^+$ Ion.* Cyclic voltammograms for the transfer of $TMA^+$ ion across the interface between a 0.1 mol $dm^{-3}$ LiCl aqueous solution and a 0.1 mol $dm^{-3}$ TBATPB nitrobenzene solution were recorded, using the two-electrode cell system shown in Fig. 1, by means of the polarographic circuit shown in Fig. 3 with the ohmic drop compensation by positive feedback. Representative cyclic voltammograms are shown in Fig. 5. Reversible cyclic voltammograms were obtained when the solution resistance was compensated for by positive feedback of $\beta=1$; the positive and negative peak potentials were independent of the $TMA^+$-ion concentration between $0.15\times10^{-3}$ and the $0.50\times10^{-3}$ mol $dm^{-3}$ and of the scan rate between 5 and 50 mV $s^{-1}$, and the peak separation was $60\pm2$ mV. The positive and negative peak currents, when corrected for the base current, were proportional to the $TMA^+$-ion concentration and to the square root of the voltage scan rate (data are not shown here). These results indicate that the two reference electrodes function as ideal non-polarized electrodes and that the ohmic drop compensation works correctly. The reversible half-wave potential, $E^r_{1/2,TMA}$ (or the midpoint potential between the positive and negative peak potentials) was determined to be $0.317\pm0.001$ V. This result agrees well with the previous result of $E^r_{1/2,TMA}=0.32$ V which was determined by potential-step chronoamperometry, cyclic voltammetry, and chronopotentiometry with a four-electrode electrochemical cell.[9]

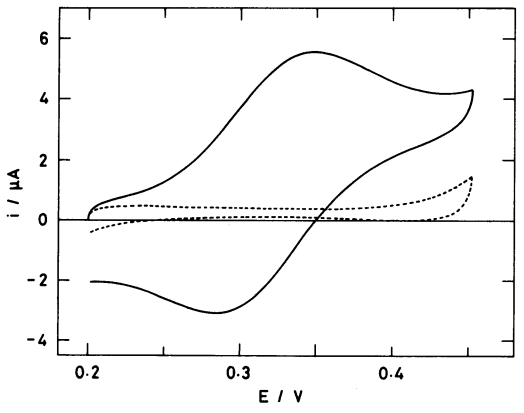


Fig. 5. Cyclic voltammogram obtained with the two-electrode cell system using the polarographic circuit as shown in Fig. 3 with positive feedback of $\beta=1$, for the transfer of $0.5\times10^{-3}$ mol $dm^{-3}$ $TMA^+$ ion from a 0.1 mol $dm^{-3}$ LiCl aqueous solution to a 0.1 mol $dm^{-3}$ TBATPB nitrobenzene solution at $v=5$ mV $s^{-1}$. Dashed line, cyclic voltammogram in the absence of $TMA^+$ ion.

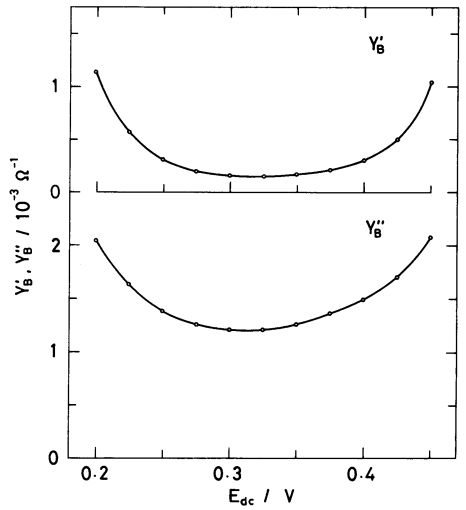


Fig. 6. Real ($Y'_B$) and imaginary ($Y''_B$) components of the base admittance at $f=50$ Hz for the interface between a 0.1 mol $dm^{-3}$ LiCl aqueous solution and a 0.1 mol $dm^{-3}$ TBATPB nitrobenzene solution.

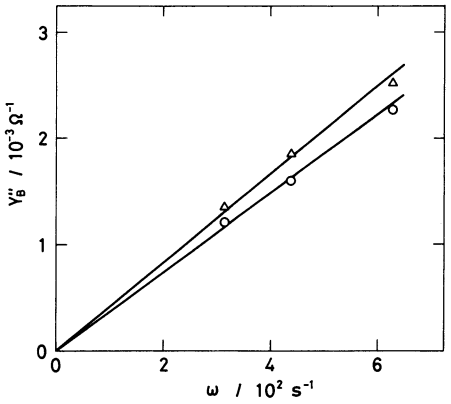


Fig. 7. Dependence of the imaginary components of the base admittance, $Y''_B$, on the angular frequency, $\omega$, at $E_{dc}=0.300$ V (○) and 0.375 V (△).

*Double-layer Capacity of Water/Nitrobenzene Interface.* Figure 6 shows an example of $Y'_B$ *vs.* $E_{dc}$ and $Y''_B$ *vs.* $E_{dc}$ curves for the interface between a 0.1 mol dm$^{-3}$ LiCl aqueous solution and a 0.1 mol dm$^{-3}$ TBATPB nitrobenzene solution. Also, as seen in Fig. 7, $Y''_B$ was proportional to $\omega$ in the frequency range between 50 and 100 Hz. From the slope of the plot of $Y''_B$ *vs.* $\omega$ the double-layer capacity of the interface, $C_{dl}$, was determined by $Y''_B = A\omega C_{dl}$. The resultant $C_{dl}$ *vs.* $E$ curve is shown in Fig. 8. The potential of the capacity minimum, $E_{min}$, was about 0.30 V. This value is close to $E_{min}$=0.29 V reported by Samec *et al.*[15] The value of $C_{dl}$ at $E_{min}$, $C_{dl,min}$, was 23.3 μF cm$^{-2}$ , which is small compared with their 27 μF cm$^{-2}$ (*cf.* Fig. 5 in Ref. 15).

Integration of the $C_{dl}$ *vs.* $E$ curve should yield the surface charge density on the water side of the interface,[8,16] $q^W$:

$$q^W = \int_{E_{pzc}}^{E} C_{dl}\, dE, \qquad (28)$$

where $E_{pzc}$ is the potential of zero charge. The value of $E_{pzc}$ has been found to be 0.265 V in the present system by electrocapillary measurement.[8,16] The resultant $q^W$ *vs.* $E$ curve is shown in Fig. 9. Also plotted in Fig. 9 are the surface charge density data obtained from the electrocapillary measurement.[8,16] The two values of $q^W$ obtained by the two different methods are in excellent agreement.

It has been shown that the residual current in the potential range between 0.20 and 0.45 V is mainly due to the transfer of $TBA^+$ and $TPB^-$ ions across the interface.[8] However, the calculated values of $Y'_B$ due to

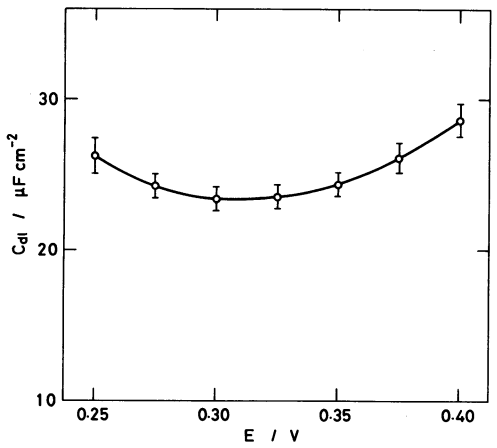


Fig. 8. Plot of the double-layer capacity, $C_{dl}$, against the potential, $E$, for the interface between a 0.1 mol dm$^{-3}$ LiCl aqueous solution and a 0.1 mol dm$^{-3}$ TBATPB nitrobenzene solution.

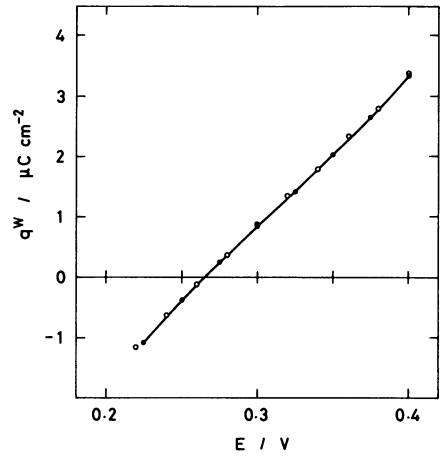


Fig. 9. Plot of the surface charge density on the water side of the interface, $q^W$, against the potential, $E$, for the interface between a 0.1 mol dm$^{-3}$ LiCl aqueous solution and a 0.1 mol dm$^{-3}$ TBATPB nitrobenzene solution, obtained by the integration of $C_{dl}$ *vs.* $E$ curve (●) and by the differentiation of the electrocapillary curve (○).[8]

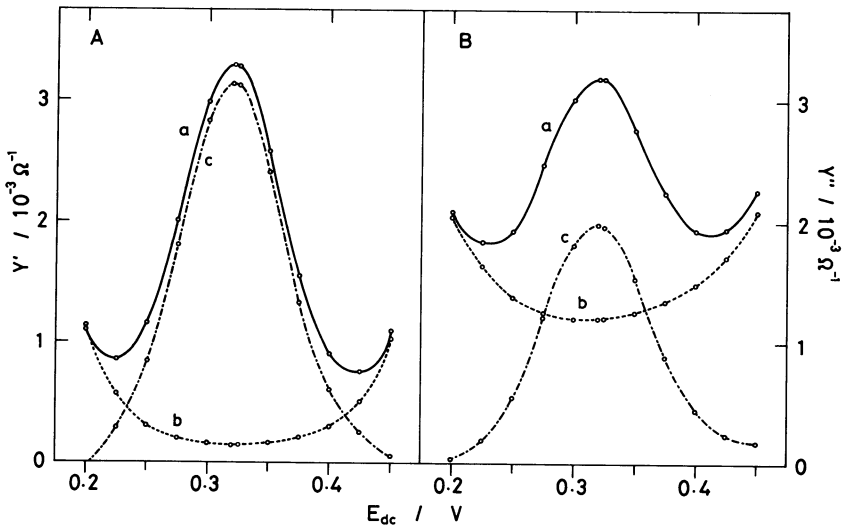


Fig. 10. Real (A) and imaginary (B) components of the admittance of the interface between a 0.1 mol dm$^{-3}$ LiCl aqueous solution and a 0.1 mol dm$^{-3}$ TBATPB nitrobenzene solution, at $f$=50 Hz, in the presence (a) and the absence (b) of 0.5×10$^{-3}$ mol dm$^{-3}$ $TMA^+$ ion in the aqueous phase. Curve c shows the ion-transfer admittance, $Y'_F$ and $Y''_F$, for the $TMA^+$-ion transfer corrected for the base admittance.

the transfer of $TBA^+$ and $TPB^-$ ion are too small to explain the observed values of $Y'_B$ (Fig. 6); for example, the calculated value of $Y'_B$ at 0.30 V and 50 Hz is $2.5\times10^{-5}$ $\Omega^{-1}$, while the observed value was $1.6\times10^{-4}$ $\Omega^{-1}$ The reason for this discrepancy is left for further study.

*Ion-transfer Impedance of $TMA^+$ Ion.* In Fig. 10 the solid lines show representative plots of $Y'_t$ and $Y''_t$ *vs.* $E_{dc}$ for the transfer of $TMA^+$ ion across the interface between a 0.1 mol $dm^{-3}$ LiCl aqueous solution and a 0.1 mol $dm^{-3}$ TBATPB nitrobenzene solution. $Y'_F$ *vs.* $E_{dc}$ and $Y''_F$ *vs.* $E_{dc}$ curves, obtained by Eqs. 2 and 3, are also shown in Fig. 10. The peak potentials of $Y'_F$ and $Y''_F$ coincided and were equal to $0.319\pm0.002$ V, irrespective of the frequency and the $TMA^+$-ion concentration, and agreed well with the reversible half-wave potential, $E^r_{1/2,TMA}=0.317\pm0.001$ V, obtained by cyclic voltammetry.

The real and imaginary components of the ion-transfer impedance, $r_s$ and $1/\omega c_s$, at $E_{dc}=0.319$ V were calculated by Eqs. 4 and 5, and plotted against $\omega^{-1/2}$ in Fig. 11. Both plots are straight lines with a common slope, which gives $D^W_{TMA}=(1.46\pm0.05)\times10^{-5}$ $cm^2$ $s^{-1}$ by Eqs. 17 and 18. This result agrees well with the previously reported value of $1.2\times10^{-5}$ $cm^2$ $s^{-1}$ determined by other electrochemical techniques.[9] Similar linear plots were also obtained for the ion-transfer impedances at several other d.c. potential in the range between 0.250 and 0.375 V.

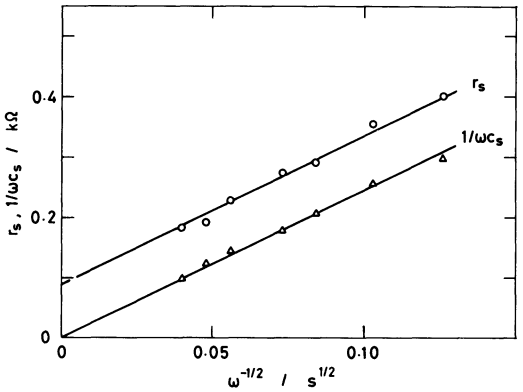


Fig. 11. Plot of the real ($r_s$) and imaginary ($1/\omega c_s$) components of the ion-transfer impedance against $\omega^{-1/2}$ for the transfer of $0.5\times10^{-3}$ mol $dm^{-3}$ $TMA^+$ ion at the interface between a 0.1 mol $dm^{-3}$ LiCl aqueous solution and a 0.1 mol $dm^{-3}$ TBATPB nitrobenzene solution at $E_{dc}=0.319$ V.

We calculated $\lambda$ from $r_s$ and $1/\omega c_s$ using Eq. 21. The results are shown in Table 1 for three different concentrations of $TMA^+$ ion. The figures are the average of the data obtained at seven different frequencies: 10, 15, 22.3, 30, 50, 70, and 100 Hz. As shown in this Table, $\lambda$ is not very dependent on the $TMA^+$-ion concentration, indicating the approximate validity of the linear kinetic equation for the ion transfer (see Eq. 22).

In Fig. 12, $\ln[\lambda/(1+\exp(-\xi))]$ is plotted against $\xi$, giving an appreciably upward convex plot, instead of a linear or nearly linear one. Frumkin correction for the double-layer effect does not reform but rather intensifies the convex nature of the plot. Formally, this convex plot can be explained by the potential dependence of the transfer coefficients. Upon assuming that $\vec{\alpha}$ varies linearly with the potential: $\vec{\alpha}=\vec{\alpha}_0+\alpha'\xi$ so that $\overleftarrow{\alpha}=\overleftarrow{\alpha}_0-\alpha'\xi=(1-\vec{\alpha}_0)-\alpha'\xi$, where $\vec{\alpha}_0$ and $\overleftarrow{\alpha}_0$ are the transfer coefficients at $\xi=0$ and $\alpha'$ is the constant, the plot was fitted to Eq. 29, a modified form of Eq. 27, by adjusting three parameters, $A'$, $\vec{\alpha}_0$ and $\alpha'$:

$$\ln[\lambda/(1+\exp(-\xi))] = \ln A' + \alpha'\xi \ln (D^W/D^N)^{1/2} + (\vec{\alpha}_0 + \alpha'\xi)\xi, \quad (29)$$

with

$$A' = k_s\left(\frac{1}{(D^W)^{1/2}}\right)^{\overleftarrow{\alpha}_0}\left(\frac{1}{(D^N)^{1/2}}\right)^{\vec{\alpha}_0}. \quad (30)$$

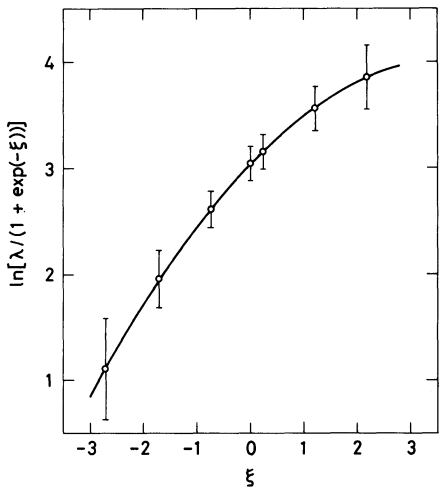


Fig. 12. Plot of $\ln[\lambda/(1+\exp(-\xi))]$ *vs.* $\xi$ $(=zF(E_{dc}-E^r_{1/2})/RT)$. The solid line shows the regression line obtained by fitting the plot to Eq. 29. Vertical bars indicate the standard deviations.

Table 1. Dependence of $\lambda$ ($s^{-1/2}$) values on the cell potential, $E_{dc}$, and the concentration of $TMA^+$ ion in the aqueous phase, $C^{W,o}_{TMA}$

| $E_{dc}$ | $C^{W,o}_{TMA}/10^{-3}$ mol $dm^{-3}$ | | | |
|---|---|---|---|---|
| V | 0.15 | 0.30 | 0.50 | Mean |
| 0.250 | 52.2(40.7)[a] | 58.2( 9.9)[a] | 48.2(12.6)[a] | 52.3(25.3)[a] |
| 0.275 | 47.8(18.4) | 50.7( 5.4) | 44.9( 8.6) | 47.8(12.2) |
| 0.300 | 41.4( 8.5) | 45.8( 3.6) | 41.6( 8.2) | 42.9( 7.1) |
| 0.319[b] | 41.2( 8.6) | 44.8( 4.0) | 40.6( 7.3) | 42.2( 6.9) |
| 0.325 | 40.4( 9.1) | 45.8( 4.1) | 40.4( 7.8) | 42.2( 7.3) |
| 0.350 | 46.9(16.0) | 51.7( 8.4) | 43.5( 6.1) | 47.3(11.0) |
| 0.375 | 50.6(18.5) | 65.5(22.1) | 50.6( 7.8) | 55.6(17.2) |

a) The figures in parentheses are the standard deviations. b) The peak potentials: $E_p=0.319\pm0.002$ V.

Regression analysis was carried out using the SALS program[17] on the FACOM M-200 Computer in the Data Processing Center of Kyoto University. The result was $A'=20.8\pm2.1\ s^{-1/2}$, $\vec{\alpha}_0=0.55\pm0.08$, and $\alpha'=-0.067\pm0.047$ by taking $D^{W}_{TMA}=1.46\times10^{-5}\ cm^2\ s^{-1}$ and $D^{N}_{TMA}=D^{W}_{TMA}/2.07=7.05\times10^{-6}\ cm\ s^{-1}$.[18] Also $k_s$ (the apparent standard rate constant) was tentatively determined to be $6.5\times10^{-2}$ cm $s^{-1}$ from $A'$. Further study is needed to find out whether the marked dependence of the transfer coefficents on the potential (as obtained here) is the common nature of the kinetic parameters of ion transfer at the interface of water and nitrobenzene (two immiscible electrolyte solutions), or a special case, indicating that the $TMA^+$-ion transfer at the 0.1 mol $dm^{-3}$ LiCl(W)/0.1 mol $dm^{-3}$ TBATPB(N) interface may involve complications which would require more complex equations of kinetics for the $TMA^+$-ion transfer in place of Eqs. 22 to 25.

In conclusion, phase-selective a.c. polarography is a promising technique for the kinetic study of the charge transfer at the interface between two immiscible electrolyte solutions.

This work was supported in part by a Grant-in-Aid from the Ministry of Education, Science and Culture.

**References**

1) C. Gavach, P. Seta, and F. Henry, *Bioelectrochem. Bioenerg.*, **1**, 329 (1974).
2) C. Gavach, B. d'Epenoux, and F. Henry, *J. Electroanal. Chem. Interfacial Electrochem.*, **64**, 107 (1975).
3) B. d'Epenoux, P. Seta, G. Amblard, and C. Gavach, *J. Electroanal. Chem. Interfacial Electrochem.*, **99**, 77 (1979).
4) Z. Koczorowski and G. Geblewicz, *J. Electroanal. Chem. Interfacial Electrochem.*, **139**, 177 (1982).
5) Z. Samec, V. Mareček, and J. Weber., *J. Electroanal. Chem. Interfacial Electrochem.*, **100**, 841 (1979).
6) Z. Samec, V. Mareček J. Weber, and D. Homolka, *J. Electroanal. Chem. Interfacial Electrochem.*, **126**, 105 (1981).
7) Z. Samec, D. Homolka, and V. Mareček *J. Electroanal. Chem. Interfacial Electrochem.*, **135**, 265 (1982).
8) T. Kakiuchi and M. Senda., *Bull. Chem. Soc. Jpn.*, **56**, 1322 (1983).
9) T. Kakutani, T. Osakai, and M. Senda, *Bull. Chem. Soc. Jpn.*, **56**, 991 (1983).
10) M. Senda, T. Kakutani, and T. Osakai., *Denki Kagaku*, **49**, 322 (1981).
11) R. Tamamushi, "Shin Jikken Kagaku Koza," ed by the Chemical Society of Japan, Maruzen, Tokyo (1977), Vol. 5, p. 370; K. Takahashi, S. Katayama, and R. Tamamushi, *Rikagaku Kenkyusho Hokoku*, **49**, 13 (1973).
12) D. C. Grahame, *J. Electrochem. Soc.*, **99**, 370C (1952).
13) M. Senda, *Kagaku No Ryoiki, Zokan*, **50**, 15 (1962).
14) M. Senda and P. Delahay, *J. Phys. Chem.*, **65**, 1580 (1961).
15) Z. Samec, V. Mareček, and D. Homolka, *J. Electroanal. Chem. Interfacial Electrochem.*, **126**, 121 (1981).
16) T. Kakiuchi and M. Senda, *Bull. Chem. Soc. Jpn.*, **56**, 1753 (1983).
17) T. Nakagawa and Y. Oyanagi, "SALS User's Manual," Computer Center of the University of Tokyo, 1979.
18) T. Osakai, T.Kakutani, Y. Nishiwaki, and M. Senda, *Bunseki Kagaku*, **32**, E81 (1983).